

XMM-Newton Observations of High Redshift Quasars ¹

D. Grupe², S. Mathur

Astronomy Department, The Ohio State University, 140 W. 18th Ave., Columbus, OH-43210, U.S.A.
 dgrupe, smita@astronomy.ohio-state.edu

B. Wilkes

Harvard-Smithsonian Center for Astrophysics, 60 Garden Street, Cambridge, MA 02138;
 email:belinda@head.cfa.harvard.edu

and P. Osmer

Astronomy Department, The Ohio State University, 140 W. 18th Ave., Columbus, OH 43210;
 posmer@astronomy.ohio-state.edu

ABSTRACT

We report on our XMM observations of the high redshift quasars BR 2237–0607 ($z=4.558$) and BR 0351–1034 ($z=4.351$). We also report on XMM observations of 19 other $z > 4$ objects available in the public archive of which 14 were detected. We find that the optical to X-ray spectral index α_{ox} is correlated with the luminosity density at 2500\AA , but does not show a correlation with redshift, consistent with earlier results. Radio loud quasars are brighter and have flatter X-ray slopes compared to radio-quiet quasars. There is some evidence for the jet dominated sources to be intrinsically absorbed. The mean intrinsic 2–10 keV power-law slope of the 10 high redshift radio-quiet quasars in our sample for which a spectral analysis can be performed is $\alpha_X=1.21\pm0.52$ (ranging between 0.32 to 1.96), more like $\alpha_X=1.19\pm0.10$ found from the ASCA observations of low redshift Narrow-Line Seyfert 1 galaxies (NLS1s), but different from $\alpha_X=0.78\pm0.11$ found for low redshift Broad-Line Seyfert galaxies. The steep X-ray spectral index suggests high Eddington ratios L/L_{Edd} . These observations give credence to the hypothesis of Mathur (2000) that NLS1s are low luminosity cousins of high redshift quasars. Comparison with other results from literature indicates that perhaps most luminous quasars, from low to high redshift, have similarly steep X-ray spectra suggestive of high Eddington luminosity.

Subject headings: galaxies: active - quasars:general - quasars: individual (BR 2237–0607, BR0351–1034)

1. Introduction

High redshift quasars can tell us about the evolution of central engines quasars, the star formation history in the early Universe (e.g., Bromm

& Larson 2004; Di Matteo et al. 2004; Granato et al. 2004; Dietrich et al. 2002a), and the intergalactic medium between the high redshift quasar and us (e.g., Storrie-Lombardi et al. 1996; Péroux et al. 2001). The high redshift quasars, however, are typically observed to be faint, making it difficult to analyze them in detail and to determine their aggregate properties. Quasars are generally classified as radio-loud (RLQ) and radio-quiet (RQQ) based on the ratio of their optical to radio luminosity (Kellerman et al. 1989). Most quasars

²Current address: Astronomy Department, Pennsylvania State University, 525 Davey Lab, University Park, PA 16802; email: grupe@astro.psu.edu

¹Based on observations with XMM-Newton, an ESA Science Mission with instruments and contribution directly funded by ESA member states and the U.S.A. (NASA).

are radio-quiet, with only about 10% being radio-loud. Additionally, a fraction of RLQs, called blazars, have strong jets pointed towards our line of sight. Many discoveries and subsequent studies of high redshift quasars were of blazars, which are relatively more bright due to their relativistically enhanced beamed emission. Naturally, results from these studies cannot be considered representative of the majority of the radio-quiet quasars. Before the Sloan Digital Sky Survey (SDSS, York et al. 2000) and the *Chandra* Deep Surveys (e.g., Brandt et al. 2001b; Giacconi et al. 2002; Barger et al. 2002; Alexander et al. 2003) only a handful of high redshift quasars were detected in X-rays. The only $z > 4$ quasar detected in X-rays before the launch of ROSAT (Trümper 1982) was GB 1508+5714 ($z=4.30$, Mathur & Elvis 1995) detected by EINSTEIN. The first X-ray selected high redshift quasar was RX J1759.4+6632 ($z=4.32$, Henry et al. 1994) found in a deep ROSAT Position Sensitive Proportional Counter (PSPC, Pfeffermann et al. 1987) observation. Only one high redshift quasar was discovered during the ROSAT All-Sky Survey (RASS, Voges et al. 1999), RX J1028.6–0844 (Zickgraf et al. 1997). Other sources were detected in X-rays, but selected in other wavelength bands, typically by their radio emission, e.g. GB 1428+4217 ($z=4.72$, Boller et al. 2000) or at optical wavelengths (e.g., Q0000–263, $z=4.111$, Bechtold et al. 1994). Up to the end of 2004 about 85 $z > 4$ quasars with X-ray detections are known ².

For the majority of these 85 quasars the number of photons detected is not sufficient to perform individual spectral analysis. As a result, derived quantities such as X-ray loudness α_{ox} ³ depend on assumptions made for spectral shape and absorbing column density. Additionally, quasar variability and lack of simultaneous optical and X-ray observations also contribute to the error on measuring α_{ox} (Strateva et al. 2005), leading to conflicting results on the properties of high redshift quasars. Studies by e.g. Wilkes et al. (1994) and Mathur et al. (2002) showed that α_{ox} depends on luminosity and not on redshift (see also Avni

& Tananbaum 1986), while studies by Brinkmann et al. (1997) and Beckmann et al. (2003) of high redshift quasars claim that α_{ox} increases with redshift. ? studied large samples stretching from low-redshift AGN to high-redshift quasars and found that the trend of α_{ox} increasing with redshift is a selection effect and that α_{ox} correlates with the luminosity density at 2500Å (see also Yuan et al. 1998a). X-ray spectroscopy is necessary to resolve these conflicting results. It has also been claimed by e.g. Elvis et al. (1994) and Cappi et al. (1997) from ROSAT and ASCA observations that high-redshift quasars show high intrinsic absorption. Recent spectroscopic observations by e.g. Ferrero & Brinkmann (2003) and Grupe et al. (2003) with XMM contradict these results. Brockopp et al. (2004) present XMM spectra of four quasars (two RLQ and two RQQ) at $z=2.96-3.77$ and find that excess absorption is present in one RLQ and one RQQ. The X-ray properties of the absorbed quasars, however, appear to be dominated by jet emission.

High-redshift quasars appear to have high mass black holes (e.g., Dietrich & Hamann 2004; Vestergaard 2004; Netzer 2003). Recent work, e.g. by Merloni (2004), suggests that high mass black holes grow rapidly, at high redshift. Mathur (2000) suggested that they are similar to low-redshift Narrow-Line Seyfert 1 galaxies (NLS1s, Osterbrock & Pogge 1985) which are objects that accrete at high Eddington ratios (e.g. Boroson 2002; ?, Grupe 2004). Like high-redshift quasars, NLS1s are also thought to be AGN in an early evolutionary state (Grupe 1996, 2004; Mathur 2000). It has also been found by Mathur et al. (2001) that NLS1s deviate from the well-known $M_{\text{BH}}-\sigma$ relation (e.g., Gebhardt et al. 2000; Ferrarese & Merritt 2000; Merritt & Ferrarese 2001) suggesting that these AGN also have rapidly growing, though smaller mass, black holes (Grupe & Mathur 2004; Mathur & Grupe 2005a,b).

To understand high redshift quasars, and to compare them to their low redshift cousins, we have initiated a program to obtain X-ray spectra of high redshift quasars using XMM-Newton. The sample consists of both radio-loud and radio-quiet quasars to probe differential evolution between the two classes, if any. We have published the results of the XMM observations of the radio-loud quasar RX J1028.6–0844 and the radio-quiet quasar BR

²A complete list of $z > 4$ quasars with X-ray detections is given at www.astro.psu.edu/users/niel/papers/highz-xray-detected.dat, Brandt et al. (2002b)

³The X-ray loudness is defined by Tananbaum et al. (1979) as $\alpha_{\text{ox}} = -0.384 \log(f_{2\text{keV}}/f_{2500\text{\AA}})$.

0351–1034 (Grupe et al. 2004). In the present paper we report the observations of the radio-quiet quasar BR 2237–0607 and a second observation of BR 0351–1034. In addition, we have selected all high redshift QSOs² with $z > 4.0$ for which public archival data could be retrieved from the XMM archive at VILSPA (December 2004). These 21 QSOs are listed in Table 1, 16 of which are RQQs, representative of the majority of the quasar population and 5 are RLQs.

The paper is organized as follows: in §2 we describe the observations and data reduction, followed by a description of the analysis of the data in §3. This Section also contains notes to individual sources. In §4 we present the results of the X-ray observation which will be discussed in §5.

Throughout the paper spectral indexes are energy spectral indexes with $F_\nu \propto \nu^{-\alpha}$. The X-ray spectral index α_X refers to the rest-frame energy range 2.0–10.0 keV, except where otherwise noted. Luminosities are calculated assuming a Λ CDM cosmology with $\Omega_M=0.3$, $\Omega_\Lambda=0.7$, and a Hubble constant of $H_0=75 \text{ km s}^{-1}\text{Mpc}^{-1}$, using the formulae by Hogg (1999). In order to determine the X-ray loudness α_{ox} we estimated the flux density at rest-frame 2500 Å from rest-frame UV spectra at 1450 Å from the literature by assuming UV spectral index $\alpha_{\text{UV}}=+0.45$ as found from composite spectra of quasars (e.g., Vanden Berk et al. 2001; Dietrich et al. 2002b). The rest-frame flux density at 2 keV was determined from the XMM pn spectra. All errors are 1σ unless stated otherwise. We also note that most of the optical and X-ray observations are separated by years.

2. Observations and Data Reduction

2.1. BR 2237–0607

The quasar BR 2237–0607 ($z=4.558$) was observed for the first time in X-rays by the ROSAT PSPC in May 1993 (Kaspi et al. 2000a). The mass of the black hole of BR 2237–0607 was estimated by Dietrich & Hamann (2004) to about $2.9 \pm 0.8 \times 10^9 M_\odot$. The black hole mass estimates are made using the virial theorem and the measurements of CIV emission line width, optical luminosity and the relationship between the luminosity and the radius of the broad emission line region (Kaspi et al. 2000b; Vestergaard

2002). Storrie-Lombardi et al. (1996) found several possible intervening damped Ly α absorption systems in the line of sight of BR 2237–0607. As per the definition of Kellermann et al. (1989), $R=10$ marks the radio-loud, -quiet division, where $R=f_{5\text{GHz}}/f_{4400\text{\AA}}$. While 5 GHz flux of BR 2237–0607 is not available in the literature, the source can be considered radio-quiet based on 1.4 GHz observations (Isaak et al. 1994).

BR 2237–0607 was observed by XMM-Newton (Jansen et al. 2001) on 2003 May 17 05:52 – 15:44 (UT) for a total of 32.5 ks with the EPIC pn (Strüder et al. 2001) and 34.2 ks with the EPIC MOS (Turner et al. 2001) detectors using thin filters. A high background flare was present during part of the exposure, especially towards the end of the observation. We excluded these times by creating a good time interval (GTI) file accepting only times when the background count rate of photons with energies $> 10 \text{ keV}$ was less than $0.1 \text{ counts s}^{-1}$. The GTI screening results in a total observing time of 23.1 ks for the pn data and of 30.0 ks for the MOS data. Source photons in the EPIC pn and MOS were collected in a circle with a radius of $25''$ and the background photons in a circle of a radius of $75''$ close by. We selected single and double events ($\text{PATTERN} \leq 4$) for the pn and single, double, triple and quadruple events ($\text{PATTERN} \leq 12$) for the MOS. Because of the much higher efficiency of the XMM XRT/pn array compared to the MOS we concentrate on the spectral analysis of the pn data and use the MOS data for consistency checks only.

For comparison purposes we also retrieved the ROSAT data from the public archive at MPE Garching. The data were analyzed by the Extended X-Ray Scientific Analysis System (EXSAS, Zimmermann et al. 1998), version 01APR⁴.

2.2. BR 0351–1034

The quasar BR 0351–1034 ($z=4.351$) was discovered with the APM high-redshift quasar survey by Irwin et al. (1991). It is radio-quiet (Isaak et al. 1994). Storrie-Lombardi et al. (1996) reported that BR0351–1034 was one of the most unusual sources in their survey of high-redshift APM Quasars with intervening absorption systems. They found saturated CIV absorp-

⁴See <http://wave.xray.mpe.mpg.de/exsas/user-guide>

tion and a large number of absorption lines associated with damped Lyman α absorption systems at $z=3.633$, 4.098 , and 4.351 . The source was first detected in X-rays by ROSAT in a 9.1 ks pointed PSPC observation with 54 ± 13 counts (Kaspi et al. 2000a). The source has been observed once before by XMM (Grupe et al. 2004). Due to high background radiation throughout, a second XMM-Newton observation was made in January 2004 and is reported here.

BR 0351–1034 was observed by XMM-Newton on 2004 January 31 12:02–21:47 (UT) for a total of 32.1 ks with the EPIC pn and 33.8 ks with the EPIC MOS detectors using thin filters. Due to high background radiation during the last half of the observation, part of the pn observation was not usable (the MOS background was much lower, so the entire exposure time was useful). The PN data were screened as discussed above, resulting in total of 23.7 ks observing time. Source counts of the pn data were collected in a circle with a radius of $20''$ and the background from a near by circular region with a radius of $40''$. Because of its small number of counts (Sect. 3.2) only the EPIC pn data with single and double events ($\text{PATTERN}\leq4$) were used for the spectral analysis. Because of the faintness of the source, proper background subtraction is important. We determined background from a second near by region as well, and found the results with the two different backgrounds to be consistent within errors.

In order to increase the signal-to-noise ratio of the spectral data, we merged the GTI screened event files of the two XMM observations of 2002-08-23 (Grupe et al. 2004) and 2004-01-31 (this work) into one event file using the XMMSAS task *merge*. The data for the spectra were selected as described above. For the background, a region was chosen which was observed on the pn CCD4 in both observations. The pn data were binned with GRPPHA to have at least 15 photons per bin. The merged data sets results in total observing times of 39.1 ks for the pn and 53.0 and 53.1 for MOS1 and MOS2, respectively. For consistency check we also fitted the spectra of the 2002 and 2004 observations simultaneously using XSPEC. The analysis and results of the first XMM-Newton observation have been discussed in Grupe et al. (2004).

2.3. $z>4$ QSOs with XMM observations

For all $z>4$ quasars found in the XMM archive we retrieved the Observational Data Files (ODF) and created the EPIC pn event files using the XMMSAS task *epchain*. The data were screened for high background radiation events using the same screening criteria as for BR0351–1034 and BR 2237–0607. All $z>4$ QSOs with XMM observations are listed in Table 1; multiple observations are available for 8 of these sources.

All XMM-Newton data were reduced using the XMM-Newton Science Analysis Software (XMMSAS) version 6.0.0 and the X-ray spectra were analyzed using XSPEC 11.3.1. The spectra were grouped by GRPPHA 3.0.0 in bins of at least 20 counts per bin, except otherwise noted. The Ancillary Response Matrix and the Detector Response Matrix were created by the XMMSAS tasks *arfgen* and *rmfgen*. In case of multiple observations, the event files were merged with the XMMSAS task *merge* and the Ancillary Response Matrices and Detector Response Matrices were combined by the FTOOLS commands *addarf* and *addrmf*, respectively. For the count rate conversions between different X-ray missions, PIMMS 3.6c was used.

3. Analysis

3.1. BR 2237–0607

3.1.1. XMM observation

During the GTI screened observations 381 ± 29 source counts were detected in the pn, 109 ± 16 counts in MOS-1, and 143 ± 18 in the MOS-2. This results in count rates of 0.0165 ± 0.0012 counts s^{-1} , $(3.67\pm0.56)\times10^{-3}$ counts s^{-1} , and $(4.77\pm0.59)\times10^{-3}$ counts s^{-1} for the pn, MOS-1, and MOS-2, respectively.

The results of the spectral analysis are given in Table 2. The data are well-fitted by a single power-law plus Galactic absorption $N_{\text{H}}=3.84\times10^{20}$ cm^{-2} (From the HI maps of Dickey & Lockman 1990). While this simple model describes the data well, with no need for excess absorption, we looked for a signature of excess absorption in the spectrum to test whether we can rule it out, and because there exist two intervening absorption systems along the line of sight of this source. Figure 1 displays the power-law fit to the pn data

(left panel) and a contour plot between the power-law slope and intrinsic N_{H} (right panel). Leaving the absorption parameter free results in a best fit value in excess of Galactic (Figure 1). The addition of absorption in excess of Galactic improves the χ^2 by 2.6 for 30 degrees of freedom, corresponding to F-test significance of $F=3.25$ and with probability $P=0.082$. An intrinsic absorber at the redshift of BR 2237–0607 results in a column density of $N_{\text{H}} = (1.84 \pm 1.50) \times 10^{22} \text{ cm}^{-2}$. A $\text{Ly}\alpha$ candidate system at $z=4.08$ and a Lyman limit system at $z=4.28$ are observed along the line of sight to BR 2237–0607 (Storrie-Lombardi et al. 1996). Due to the limited S/N of the spectrum, however, the redshift of the absorber is not constrained. If the absorber redshift corresponds to the 2 intervening absorbers, the implied column density is $N_{\text{H}} = (1.6 \pm 1.4) \times 10^{22} \text{ cm}^{-2}$ ($z=4.28$) and $N_{\text{H}} = (1.5 \pm 1.2) \times 10^{22} \text{ cm}^{-2}$ ($z=4.08$). This column density is a factor of about 50 larger than $N_{\text{HI}} = (2.5) \times 10^{20} \text{ cm}^{-2}$ estimated by Storrie-Lombardi et al. (1996) for the $\text{Ly}\alpha$ system at $z=4.08$, and would imply unusually large abundances for the intervening systems. Even though the errors on X-ray column density measurements are large, the intervening absorption is excluded at more than 3σ . Therefore, we conclude that the additional absorption, if present, is intrinsic to the quasar and not to an intervening system. We reiterate, however, that the possibility of intrinsic absorption is only a 1σ result.

The rest-frame unabsorbed 2.0–10.0 keV flux is $2.6 \times 10^{-17} \text{ W m}^{-2}$ ($2.6 \times 10^{-14} \text{ ergs s}^{-1} \text{ cm}^{-2}$) which gives a rest-frame 2–10 keV luminosity of $\log L_{2-10 \text{ keV}}=38.68$ [W] (45.68 [ergs s^{-1}]). From the rest-frame UV spectrum (Dietrich et al. 2003) and the power law fit to the pn data we derived an X-ray loudness $\alpha_{\text{ox}}=1.58 \pm 0.08$.

3.1.2. Comparison with ROSAT

From the 9.4 ks ROSAT PSPC observation we measured 37.0 ± 14.1 photons corresponding to a count rate of $(3.92 \pm 1.48) 10^{-3} \text{ counts s}^{-1}$ in the 0.1–2.0 keV band. However, this is a factor of about 1.5 lower than that reported previously by Kaspi et al. (2000a) who gave a PSPC count rate $= (6.2 \pm 1.4) 10^{-3} \text{ counts s}^{-1}$. We tried different background regions in order to search for differences in the background subtraction, but found this not to be the cause. Our measured count

rate, however, is consistent with the count rate of $(2.94 \pm 0.67) 10^{-3} \text{ counts s}^{-1}$ given in the ROSAT source catalogue and in Vignali et al. (2001), which support the results of our analysis. The PSPC count rate is a factor of about 1.6 higher than expected, based on the pn count rate. However, due to the low number of PSPC photons and the associated error, the source flux is constant within 2σ .

From the ROSAT PSPC data we measured a hardness ratio⁵ $\text{HR}=0.37 \pm 0.34$. The hardness ratio derived from the XMM pn spectrum with a power law model with Galactic and intrinsic absorption as given in Table 2 suggests a much harder spectrum with $\text{HR}=0.82$. On the other hand, if we use the power law model ($\alpha_{\text{X}}=0.87$) with Galactic absorption only, the resulting $\text{HR}=0.52$ which is consistent with the HR measured from the PSPC. We also checked if additional information is obtained by subdividing the PSPC energy range to define two hardness ratios HR1 and HR2 ⁶. We again found that the observed values are more consistent with a model containing Galactic absorption only rather than that with excess absorption. The softer spectrum and higher count rate during ROSAT observation suggest that the BR2237–0607 spectrum is variable, but the limited S/N of both XMM and ROSAT spectra do not allow us to draw any firm conclusions.

3.2. BR 0351–1034

The mean count rates during the 2004 January observations are $(5.38 \pm 0.03) 10^{-3} \text{ counts s}^{-1}$ for the EPIC pn, and $(2.12 \pm 0.41) 10^{-3} \text{ counts s}^{-1}$ and $(1.37 \pm 0.37) 10^{-3} \text{ counts s}^{-1}$ for the EPIC MOS 1 and 2, respectively. This results in total numbers of background subtracted source counts of 127 ± 22 for the pn and 71 ± 14 and 44 ± 12 for the MOS 1 and 2. The count rates are similar to those obtained during the first XMM observation on 2002 August 23 (Grupe et al. 2004). The merged spectra of the 2002 August and 2004 January observations have a total of 234 ± 30 , 98 ± 18 , and 86 ± 18 source counts for the pn, MOS1, and MOS2, respectively. The number of counts in the

⁵The hardness ratio is defined as $\text{HR}=(\text{H}-\text{S})/(\text{H}+\text{S})$ with soft band S in the energy range 0.1–0.4 keV and H between 0.5–2.0 keV

⁶The HR1 is same as HR defined above and HR2 is between soft and hard bands of 0.5–0.9 and 0.9–2 keV respectively.

pn detector are sufficient to perform a basic spectral analysis; therefore, we focus on the merged pn data only.

Figure 2 displays powerlaw fits to the 2004 January and the 2002+2004 merged data including contour plots between the intrinsic N_H and the photon index Γ . Table 3 summarizes the results of spectral fits to the EPIC pn data of BR 0351–1034. Since the results of the spectral analysis of the 2004 January and the merged data from the 2002 August and 2004 January data are consistent, we discuss the merged data here. The merged data are consistent with a power law with the absorption parameter set to the Galactic value $N_H=4.08 \times 10^{20} \text{cm}^{-2}$, with best fit power-law slope $\alpha_X=0.42 \pm 0.17$. Leaving the absorption parameter free results in an absorption column at $z=0$ of $1.0 \pm 0.9 \times 10^{21} \text{cm}^{-2}$. Thus, even though the best fit column density implies absorption in excess to the Galactic, this is not a secure result because of the large error on N_H . If the absorber is placed at the redshift of the quasar the fit results in an upper limit of the absorption column of $2.9 \times 10^{22} \text{cm}^{-2}$. With the absorbing column fixed at Galactic, the power-law spectral index is $\alpha_X=0.42 \pm 0.17$, unusually flat for a radio-quiet quasar. On the other hand, ROSAT data suggest a steep spectral slope with $\alpha_X=3.5$ (see Grupe et al. 2004a for a detailed discussion on comparison with ROSAT data). Motivated by these results, we fitted the merged data with a broken power-law model with $\alpha_{X,soft}=3.5$. The resulting fit is good, with $\alpha_{X,hard}=1.42 \pm 0.18$, but the data quality is not good enough to favor one fit over others (see Table 3). For comparison purposes we also fitted the 2002 August and 2004 January data simultaneously in XSPEC. As shown in Table 3, we do not find significant differences between the fits to the merged data set or the simultaneous fits to the 2 single data sets.

The absorption corrected rest-frame 2–10 keV flux of the merged spectrum is $\log F_X = -17.1$ [W m^{-2} (-14.1 [$\text{ergs s}^{-1} \text{cm}^{-2}$]). This flux converts to an unabsorbed rest-frame 2–10 luminosity 38.13 [W] (45.13 [ergs s^{-1}]). The X-ray loudness is $\alpha_{ox}=1.59 \pm 0.08$ using the rest-frame UV spectrum given in Storrie-Lombardi et al. (1996). We note that Kaspi et al. (2000a) and Vignali et al. (2001) quote α_{ox} of 1.35 and 1.6 respectively.

3.3. High-redshift QSOs with XMM observations

Here we describe the analysis of all high-redshift quasars with XMM observations publicly available (December 2004). All these sources are listed in Table 1. If enough photons were collected for a source we performed a power law fit with Galactic absorption and intrinsic absorption if needed by the data. The results of these fits and the rest frame 2–10 keV fluxes and luminosities are given in Table 4. All EPIC pn spectra are shown in Figure 3. Several sources have less than 100 detected counts, resulting in only approximate X-ray spectral slopes; α_X derived from these datasets should be treated with caution. The errors given for α_{ox} were estimated from the errors in the X-ray spectral index and the normalization of the spectrum. This is a lower limit of the error, because it does not take into account errors in the optical spectrum, e.g. we assume a general optical/UV slope of $\alpha_{UV}=0.45$ (e.g., Vanden Berk et al. 2001) and Dietrich et al. (2002b). Another source of errors in the optical spectrum is reddening which is difficult to compute.

3.3.1. Q 0000–2619

The XMM observation of the $z=4.1$ radio-quiet quasar Q 0000–2619 (e.g. Bechtold et al. 1994) was discussed in detail in Ferrero & Brinkmann (2003). The pn spectrum is well fitted by a single powerlaw with Galactic absorption. Adding an intrinsic absorber at the redshift of the quasar does not improve the fit and the column density can not be constrained. The best fit power-law slope is $\alpha_X=1.15 \pm 0.06$. The X-ray loudness $\alpha_{ox}=1.82 \pm 0.03$ was determined from the dereddened rest frame UV spectrum given in Bechtold et al. (1994) and the rest-frame 2 keV flux determined from the pn spectrum. This value agrees, within errors, with the $\alpha_{ox}=1.85$ given in Ferrero & Brinkmann (2003) and Bechtold et al. (1994), but differs from $\alpha_{ox}=1.65$ and $\alpha_{ox}=1.71$ derived from ROSAT data reported in Kaspi et al. (2000a) and Vignali et al. (2001) respectively. The ROSAT data presented by Kaspi et al. (2000a) contained only 180 counts. While this was a secure detection, the power-law slope of the spectrum was not as well determined as from the XMM spectrum, and so α_{ox} was not well de-

terminated; different optical slopes also contribute towards different values of α_{ox} .

3.3.2. *SDSS 0040-0915*

The $z=4.98$ radio-quiet quasar SDSS 0040-0915 (Schneider et al. 2003) was serendipitously observed by XMM during a 9ks observation of the galactic cluster Abell 85 (Durret et al. 2005). The 50 photons detected during this observation only allow a rough estimate of the spectral slope of the X-ray spectrum. The data were rebinned in groups of at least 10 counts per bin. The absorption parameter was fixed to the Galactic value which is consistent with the data. The data can be fitted by a single power law with $\alpha_X = 1.43 \pm 0.34$. The X-ray loudness $\alpha_{\text{ox}} = 1.39 \pm 0.14$ was estimated from the rest-frame UV spectrum given in Schneider et al. (2003) and the pn spectrum and is in agreement within the errors with $\alpha_{\text{ox}} = 1.55$ given in Schneider et al. (2003). The steeper X-ray loudness found by Schneider et al. (2003) can be explained with their assumption of an X-ray spectral index $\alpha_X = 1.0$ and the lower count rate and therefore lower flux in the pn energy band. Also note that Schneider et al. (2003) use an UV spectral slope $\alpha_{\text{UV}} = 0.79$ to extrapolate to the flux density at rest frame 2500Å.

3.3.3. *BRI 0103+0032*

This $z=4.44$ radio-quiet quasar (Smith et al. 1994, Stern et al. 2000) was observed by XMM for only 4ks. Only 50 source photons were detected during the observation, allowing only a rough spectral fit with a powerlaw model with $\alpha_X = 1.96 \pm 0.50$ and the absorption parameter fixed to the Galactic value. The data do not indicate additional intrinsic absorption. This is the steepest α_X known for a high redshift quasar. Even if the actual value of α_X is lower by 1σ , it is still very steep, comparable to that of NLS1 galaxies at low redshift (Figure 6). The X-ray loudness $\alpha_{\text{ox}} = 1.41 \pm 0.36$ given in Table 4 was derived from the rest-frame UV spectrum (Dietrich et al. 2003) and the XMM EPIC pn X-ray data.

Dietrich & Hamann (2004) give a black hole mass of $1.0 \pm 0.3 \times 10^9 M_\odot$ and an Eddington ratio $L/L_{\text{Edd}} = 3.5$; the black hole mass was determined using the CIV emission line width and the broad line region radius–luminosity relation as

mentioned above. This high L/L_{Edd} may explain the steep X-ray spectrum of the source; L/L_{Edd} and α_X have been found to be closely correlated in low-redshift AGN (Grupe 2004, Williams et al. 2004). Even though black hole masses derived from C IV and Mg II widths are highly uncertain, even an order of magnitude lower L/L_{Edd} is still high, comparable to that of low redshift NLS1s.

3.3.4. *PSS J0248+1802*

The $z=4.422$ quasar PSS J0248+1802 was discovered by Kennefick et al. (1995) from a multi-colour survey using the Second Palomar Observatory Sky Survey. This radio-quiet quasar (Stern et al. 2000) has been a target of Chandra (Vignali et al. 2001) as well as XMM. It was observed by XMM in February 2003 for a GTI screened time of 7.4 ks (Table 1) yielding 160 photons. The data were grouped in bins of at least 15 counts per bin. A fit to the pn data is consistent with a single powerlaw with $\alpha_X = 1.10 \pm 0.15$ with Galactic absorption. Vignali et al. (2001) suggested from the Chandra observation that the source seem to be intrinsically absorbed with a column density larger than $5 \times 10^{23} \text{cm}^{-2}$. However, this claim was based on only 19 source photons and is not supported by XMM data; the best fit value of intrinsic absorption is an upper limit $N_{\text{H}} = 3 \times 10^{20} \text{cm}^{-2}$ (90% error). We estimate the X-ray loudness $\alpha_{\text{ox}} = 1.47 \pm 0.07$ from the optical/UV spectrum (Dietrich et al. 2003) and the pn spectrum. The black hole mass was measured by Dietrich & Hamann (2004) to be $(6.6 \pm 1.6) \times 10^9 M_\odot$ with an Eddington ratio $L/L_{\text{Edd}} = 0.91$.

3.3.5. *PMN J0525-3343*

The XMM observations of the blazar PMN J0525-3343 ($z=4.40$) have been presented and discussed in detail in Worsley et al. (2004a) who reported the presence of a warm absorber in this source, confirming a claim based on BeppoSAX observations (Fabian et al. 2001). Table 5 summarizes the observations which we merged into one event file. Note that the GTI screened times given in Table 5 deviate from the ones given in Table 1 in Worsley et al. (2004a). The reason is a different screening for the Good Time Intervals (M. Worsley, 2004, priv. comm.). We did not use the observations performed during orbits 603 and 608

due to very high background radiation throughout those orbits.

A single power-law fit to the data with the absorption column density fixed to the Galactic value $N_H = 2.21 \times 10^{20} \text{ cm}^{-2}$ as given in Table 1 does not give an acceptable fit ($\chi^2/\text{dof} = 927/601$). The result suggests intrinsic absorption at the redshift of the quasar. Adding an absorber at the location of the quasar significantly improved the fit. The best fit results in an intrinsic cold absorber with $N_H = 1.6 \times 10^{22} \text{ cm}^{-2}$ and an X-ray spectral slope $\alpha_X = 0.71 \pm 0.01$, which agrees with the value given by Worsley et al. (2004a) (0.67 ± 0.03); an additional warm absorber was not required by the data (see residuals to the fit in Figure 3).

PMN J0525–3343 shows a slight increase in its EPIC pn count rate from $0.311 \pm 0.006 \text{ counts s}^{-1}$ during the February 2001 observation to $0.457 \pm 0.008 \text{ counts s}^{-1}$ during the August 2003 observation. The X-ray loudness $\alpha_{\text{ox}} = 1.04 \pm 0.01$ was estimated from the R magnitude measured from the APM scans given in Péroux et al. (2001) and the pn spectrum. There is a large uncertainty in determine α_{ox} for PMN J0525–3343, because we do not know the optical reddening. The intrinsic absorption column $N_H = 1.6 \times 10^{22} \text{ cm}^{-2}$ suggests that the source may be reddened in the optical. However, the source is detected in the rest-frame UV, suggesting that the reddening is not severe. In order to determine the reddening NIR spectra are needed to measure the Balmer-decrement.

3.3.6. *RX J1028.6–0844*

The $z=4.276$ radio-loud quasar RX J1028.6–0844 was the only $z>4$ quasar discovered during the RASS (Zickgraf et al. 1997). From a long ASCA observation, Yuan et al. (2000) suggested that the quasar is intrinsically highly absorbed ($N_H = 2 \times 10^{23} \text{ cm}^{-2}$). However, a 4.4 ks observation with XMM did not confirm the presence of a strong intrinsic absorber (Grupe et al. 2004). Due to the capability of the EPIC pn to observe down to low X-ray energies of 0.2 keV, Grupe et al. (2004) measured the intrinsic absorption column N_H of at most a few times 10^{22} cm^{-2} . From a ten times longer XMM observation Yuan et al. (2005) confirmed that indeed, the source is not as highly absorbed as claimed from the ASCA data; the best fit intrinsic cold absorption is $N_H = 2.1_{-0.3}^{+0.4} \times 10^{22} \text{ cm}^{-2}$. Yuan et al. (2005)

argue for an additional warm absorber with column density $N_H > 2 \times 10^{22} \text{ cm}^{-2}$.

3.3.7. *SDSS J1030+0524*

Petric et al. (2003) found an upper limit of the radio flux at 1.4 GHz $S_{1.4\text{GHz}} < 61 \mu\text{Jy}$ which makes this source radio-quiet. With a redshift of $z=6.28$ SDSS J1030+0524 is currently the quasar with the highest redshift detected in X-rays. The quasar was detected by Chandra (Mathur et al. 2002; Brandt et al. 2002a). It was also observed by XMM in May 2003 (Farrah et al. 2004) for 67 ks with the pn (Table 1) resulting in 340 source counts. While a spectral fit to the pn data with only Galactic absorption provides a good fit ($\chi^2/\nu=39/40$), the fit improves significantly with the addition of intrinsic absorption of $6.5 \pm 3.7 \times 10^{22} \text{ cm}^{-2}$ ($\chi^2/\nu=32/39$). An F-test results in an F-test value 8.4 with a probability $P=0.006$. The X-ray spectral slope $\alpha_X = 1.65 \pm 0.34$ is one of the steepest in the high-redshift quasar sample presented here. These results are consistent with those of Farrah et al. (2004) within 2σ errors.

3.3.8. *BRI 1033–0327*

The $z=4.49$ quasar BRI 1033–0327 has been found by Isaak et al. (1994) to be radio-quiet. The 55.7 ± 13.6 counts found in the 26.5 ks pn observation of BRI 1033–0327 allow only a very rough spectral fit to the data. The data were binned with at least 10 counts per bin and are consistent with a simple power law with $\alpha_X = 1.34 \pm 0.47$ and Galactic absorption (Table 4). The X-ray loudness $\alpha_{\text{ox}} = 1.80 \pm 0.20$ was estimated from the rest-frame UV spectrum shown in Storrie-Lombardi et al. (1996) and the fit to the pn data. Given the correlation between α_{ox} and optical luminosity (figure 4; Strateva et al. 2005), large values of α_{ox} are expected in highly optically luminous quasars. BRI 1033–0327, however, is not very luminous, with $\log l_{2500\text{\AA}} = 24.68$ (luminosity density in W Hz^{-1} ; Table 4), making the source unusually X-ray weak. Note, that the error on α_{ox} is large. Moreover, even though the data are consistent with Galactic absorption only, strong intrinsic absorption can not be excluded. This would result in underestimating the intrinsic X-ray luminosity as well as the power-law slope.

3.3.9. *SDSS J1044-0125*

This $z=5.74$ quasar was discovered by Fan et al. (2000) and has been found to be radio-quiet (Petric et al. 2003). It was clearly detected by XMM in May 2000 with 31.7 ± 8.5 counts in the observed 0.5-2.0 keV range in the pn (Brandt et al. 2001a). The XMM data have been analyzed and discussed in detail by Brandt et al. (2001a) and ?. The ≈ 30 photons in this XMM observation do not allow any direct spectral analysis. ? performed a hardness ratio analysis and argued that the intrinsic X-ray spectral slope may be steep with $\alpha_X=1.5$ absorbed by a partially covering absorber.

3.3.10. *RX J1052.4+5719*

This high-redshift quasar ($z=4.45$) was discovered from ROSAT observations (Schneider et al. 1998) of the Lockman Hole (Hasinger et al. 1998). We used all XMM observations as listed in Worsley et al. (2004c) for which RX J1052.4+5719 was in the field-of-view, using the medium filter (Table 6). From the screened event files we created a merged event file with a total observing time of 535 ks (this is the total observing time; the exposure time at the source is smaller by about a factor of two). At the position of the source we found 368 ± 52 source photons. Although the number of photons would suggest good spectral data, this is not the case for RX J1052.4+5719 due to the high background in the XMM EPIC-pn detector. The observed count rate is low, 6.88×10^{-4} counts s^{-1} , so the data are dominated by background in the pn detector. We fitted a single absorbed powerlaw to the data with the absorption column density fixed to the Galactic value. The fit results in a relatively steep energy spectral slope $\alpha_X=1.58 \pm 0.30$ and does not require any additional intrinsic absorption.

We estimated an optical/UV – X-ray spectral index $\alpha_{ox}=1.20 \pm 0.15$ from spectrum given in Schneider et al. (1998) and the pn spectrum presented here. The actual, exposure corrected α_{ox} is somewhat smaller, about $\alpha_{ox}=1.08 \pm 0.15$. Kaspi et al. (2000a) reported that RX J0152.4+5719 was not detected in the NVSS radio survey (Cordon et al. 1998) and gave an upper limit for the radio loudness of $R < 190$. This makes it difficult to determine whether RX J1052.4+5719 is a radio-loud or a radio-quiet quasar; the X-ray spectral

index $\alpha_X=1.58$ suggests that it is radio-quiet.

3.3.11. *HDF-N objects*

Three spectroscopically confirmed AGNs were detected in the Hubble Deep Field North (HDF-N) by Chandra: VLA J1236+6213, CXOHDFN J123647.9+620941, and CXOHDFN J123719.0+621025 (Brandt et al. 2001b; Barger et al. 2002). This field has also been the target of several XMM observations (Table 7). The merged event file of these observations results in a background screened total observing time of 205 ks (Table 7). However, due to the significantly higher background in the EPIC pn detector compared to Chandra’s ACIS-S, and the much shorter observing time with XMM, none of the three source could be detected above the background.

3.3.12. *CXOCY J125304-090737*

The $z=4.180$ quasar CXOCY J125304-090737 was discovered by Castander et al. (2003) in a 49.2 ACIS-S observation of the Hickson group of galaxies HCG 62. It was also observed serendipitously in the field of view during an 8 ks XMM observation of HCG 62, but we did not detect the source. Converting the ACIS-S count rate into EPIC pn assuming $\alpha_X=0.7$ and the Galactic absorption column density $3 \times 10^{20} \text{ cm}^{-2}$ as given in Castander et al. (2003) results in 0.0011 pn counts s^{-1} . This low count rate in the pn would be dominated by the detector background. We would have expected to detect only about 8 source photons during the entire XMM observation, which explains the non-detection in the pn.

3.3.13. *SDSS J1401+0244*

The $z=4.38$ quasar SDSS J1401+0244 was serendipitously observed by XMM in an observation of the galactic cluster A 1835 (Schneider et al. 2003). We measured 115 ± 20 source counts at the position of the source allowing us for a rough analysis of the X-ray spectrum. The pn spectrum can be fitted with a very flat X-ray spectrum with $\alpha_X=0.32 \pm 0.39$ and Galactic absorption. As suggested by Schneider et al. (2003) there is no evidence of intrinsic X-ray absorption in SDSS J1401+0244. The radio-loudness of SDSS J1401+0244 is uncertain. From the FIRST radio survey (Becker et al. 1995) we get a 5σ upper

limit of 0.95 mJy. With an i-magnitude $i=18.6$ mag (Schneider et al. 2003) we can derive an upper limit of the radio-loudness to $R<100$. The rather flat X-ray spectrum of this quasar suggests that it is a radio-loud quasar while the X-ray loudness $\alpha_{\text{ox}}=1.77$ (Schneider et al. 2003) suggests it is radio-quiet. Deeper radio observations of SDSS J1401+0244 are necessary to clarify the radio nature of this source. Because we do not have any evidence that the source is radio-loud we tentatively consider it to be radio-quiet. Alternatively, the intrinsic X-ray spectrum may be complex, but appears simple in the low S/N data, leading to underestimating the true flux.

3.3.14. GB 1428+4217

The radio-loud $z=4.72$ quasar GB 1428+4217 was discovered by Hook & McMahon (1998) and was a target of several X-ray satellites (Fabian et al. 1997 (ROSAT); 1998 (ASCA); Boller et al. 2000 (ROSAT)). GB 1428+4217 was actually the last source ever observed by ROSAT in December 1998 (Boller et al. 2000). It was recently observed also by XMM (Worsley et al. 2004b). Spectral fits to the pn data of GB 1428+4217 are consistent with a power law with Galactic and intrinsic absorption, confirming earlier results from ROSAT and ASCA (Boller et al. (2000) and Fabian et al. (1998), respectively). The best-fit power-law slope is $\alpha_X = 0.86 \pm 0.03$. While Fabian et al. (2001) argue for the presence of an intrinsic warm absorber, a fit with cold absorption describes the XMM data well, with $N_H = 2.13 \pm 0.23 \times 10^{22}$ atoms cm^{-2} . The X-ray loudness $\alpha_{\text{ox}}=0.84 \pm 0.01$ was determined from the flux density at 8550\AA ($=1500\text{\AA}(1+z)$) given in Hook & McMahon (1998) and the pn X-ray spectrum.

3.3.15. GB 1508+5714

The $z=4.3$ radio-loud quasar GB 1508+5714 was discovered in X-rays from an Einstein observation by Mathur & Elvis (1995). From Chandra ACIS-S observations Yuan et al. (2003) and Siemiginowska et al. (2003) reported the discovery of an X-ray jet which was also detected in radio at 1.4 GHz with VLA observations (Cheung 2004). GB 1508+5714 was observed twice by XMM during orbits 443 and 529 on 2002 May 11 and 2002 Oct 30. However, due to very high

background radiation during the second observation, only the 2002 May 11 observation is useful. The jet is not resolved in XMM data, so the XMM spectrum is a combined spectrum of the core and the jet. The flux in jet is only $\sim 2\%$ of the core flux; therefore the combined spectrum is dominated by the core component of the quasar itself. This is clearly seen by the fact that the spectral fit to the pn data results in a power law with $\alpha_X=0.55 \pm 0.04$ and Galactic absorption, compared to $\alpha_X=0.55 \pm 0.06$ found with Chandra data (Siemiginowska et al. 2003). Adding an intrinsic absorber to the model does not improve the fit. The X-ray loudness $\alpha_{\text{ox}}=1.07 \pm 0.02$ was determined from the UV spectrum given in Storrie-Lombardi et al. (1996) and the pn spectrum given in Table 4.

3.3.16. RX J1759.4+6838

The $z=4.32$ quasar RX J1759.4+6838 was the only X-ray selected $z>4$ quasar that was discovered by ROSAT in a long PSPC observation of the North Ecliptic Pole (Henry et al. 1994). The source was serendipitously observed during two EPIC pn observations of NGC 6552 (Table 1). Assuming an unabsorbed flux of $\log F_{0.5-2.0 \text{ keV}} = -17$ [W m^{-2}] (-14 [$\text{ergs s}^{-1} \text{ cm}^{-2}$]) as given by Henry et al. (1994) and a powerlaw with $\alpha_X=1$ and absorption with a column density $N_H = 4 \times 10^{20} \text{ cm}^{-2}$ we would have detected about 40 source counts during the effective 5.9 ks (measured from the combined exposure map). However, the XMM observation only results in 11.5 ± 6.9 pn counts suggesting that either the spectral shape, normalization or the absorption changes by on a time scale of about 2 years (rest-frame), resulting in a factor of 4 change in the observed flux. Kaspi et al. (2000a) estimated the radio-loudness $R=30$ which makes this source a moderately radio-loud quasar as per the definition of Kellermann et al. (1989).

3.3.17. CXOMP J213945-234655

This $z=4.93$ quasar was discovered by Silverman et al. (2002) through the Chandra Multiwavelength Project (ChAMP, Wilkes et al. (2001)). The source was detected on the Chandra ACIS-I detector with 16.7 ± 7.7 counts in the observed 0.3-2.5 keV range during a 41 ks observation. CXOMP J213945-234655 was also observed

by XMM serendipitously during a 12 ks observation of MS 2137–23. We could not detect any source at the position of CXOMP213945–234655 due to the low flux of the source and the higher instrumental background of the pn compared to ACIS-S. There is no source in the NVSS (Cordon et al. 1998) at the position of CXOMP J213945–234655. Deeper radio observations at the position of CXOMP J213945–234655 are necessary to clarify whether it is a radio-loud or radio-quiet quasar. The X-ray loudness $\alpha_{\text{ox}}=1.52$ (Silverman et al. 2002) suggests a radio-quiet nature.

4. Results

4.1. BR 2237–0607

Our spectral analysis of the pn data of BR 2237–0607 has shown that it does not show significant intrinsic absorption, if present at all. This result is in agreement earlier findings from XMM data, by e.g. Ferrero & Brinkmann (2003, for radio-quiet quasars) and Grupe et al. (2004a, for radio-loud and -quiet quasars), that high-redshift quasars are not intrinsically more absorbed than low redshift AGNs.

Dietrich & Hamann (2004) estimated the mass of the central black hole to be $2.9 \pm 0.8 \times 10^9 M_{\odot}$ which corresponds to an Eddington Luminosity of $\log L_{\text{Edd}}=39.4$ [W]. The bolometric luminosity $\log L_{\text{bol}} = 39.7$ [W] implies an Eddington ratio L/L_{Edd} of about 2 and requires a mass accretion rate of $10 M_{\odot}\text{yr}^{-1}$. However, even if L/L_{Edd} is lower by factors of several, it would be still high, comparable to those found among low-redshift NLS1s (e.g. Grupe 2004). Typically NLS1s have Eddington ratios L/L_{Edd} in the order of 1, while Broad Line Seyfert 1s have L/L_{Edd} about 1 or 2 orders of magnitude smaller (See Figure 13 in Grupe 2004).

We can estimate a FWHM($H\beta$) of BR 2237–0607 from the bolometric luminosity using the relation by Kaspi et al. (2000b). This results in $\text{FWHM}(H\beta) \approx 4500 \text{ km s}^{-1}$. This is clearly much larger than the 2000 km s^{-1} boundary used to define NLS1s at low redshift. The definition of “narrowness” of FWHM($H\beta$), should be a function of luminosity. Only then can we meaningfully expand the NLS1 class to narrow-line quasar, to include all highly accreting objects. This result is similar in spirit with recent results from Corbett

et al. (2003) and Shemmer et al. (2004). Using data from 2dF quasar redshift survey, Corbett et al. have found that the width of the $H\beta$ line correlates with luminosity, leading to the correlation of BH mass with luminosity. Similarly, Shemmer et al. have found that the Eddington luminosity ratio is proportional to the 0.4 power of luminosity and inversely proportional to the square of $H\beta$ width. Thus, quasars with high Eddington luminosity can have broader $H\beta$ width, dependent on luminosity.

4.2. BR0351–1034

The spectral analysis of the second XMM observation from January 2004 of the radio-quiet quasar BR 0351–1034 are in agreement with our earlier results from the August 2002 observation (Grupe et al. 2004). In both cases the data are consistent with a single powerlaw with Galactic absorption. The merged data sets also yield similar results. As discussed in §3.2, a broken power-law appears to be an appropriate spectral model for this source (Table 3). Such a steep soft X-ray spectrum with $\alpha_{\text{X}}=3.5$ would suggest that BR 0351–1034 is an AGN with a high Eddington ratio L/L_{Edd} following the correlation between X-ray spectral index and L/L_{Edd} found among low-redshift AGNs by Grupe (2004) and narrow line Seyfert 1s by Williams et al. (2004). The hard X-ray power-law slope is 0.42 ± 0.18 with only Galactic absorption and is 0.67 ± 0.21 allowing for intrinsic absorption (Table 3). However, intrinsic absorption is not required.

4.3. $z > 4$ quasars

Figure 4 displays the relation between the X-ray spectral index α_{X} and the X-ray loudness α_{ox} . As expected from earlier results by e.g. Wilkes & Elvis (1987) the radio-loud quasars have much flatter X-ray spectra and smaller α_{ox} than the radio-quiet AGNs, similar to that observed at low redshift. We did not find a clear correlation between α_{X} and α_{ox} among the radio-quiet AGN. There is, however, a mild trend that sources with steeper X-ray spectra tend to be stronger in X-rays, i.e. have smaller α_{ox} ($r_s = -0.40$, $T_s = -1.2$, $P=0.26$). For our high redshift quasars the observed XMM energy range of 0.2–10 keV corresponds to a rest frame range of ≈ 1 –55 keV. It is therefore important to compare the α_{X} values of

our sample to the hard X-ray power-law slopes of low redshift AGNs, as observed by ASCA. The dashed-dotted lines mark the mean value of the 2-10 keV X-ray slope α_X of low-redshift NLS1s (23 sources) and BLS1s (17 sources) of the ASCA sample of Leighly (1999). Most of the high-redshift radio-quiet AGN of our sample have similar steep X-ray slopes as NLS1s, suggesting similar high Eddington ratios L/L_{Edd} . The X-ray spectral slopes of radio-quiet AGN with X-ray spectra in our sample ranges between 0.32 to 1.96 and gives a mean $\langle \alpha_X \rangle = 1.21 \pm 0.52$ which compares to $\langle \alpha_X \rangle = 1.19 \pm 0.10$ found by Leighly (1999) for low-redshift NLS1s. The mean α_X of the low redshift broad line Seyfert 1s, on the other hand, is 0.78 ± 0.11 (Leighly 1999). These values are similar to the ones found by Brandt et al. (1997) for low redshift Seyferts. One should be careful, however, in comparing the spectral shape of our high redshift quasar sample to low redshift Seyfert galaxies. The X-ray spectra of Seyferts often show complex shapes including warm absorbers and Compton reflection components. If the reflection component is not modeled properly, the underlying power-law slope may be underestimated. As shown in Brandt et al. (1997), however, the error introduced is only of the order of $\Delta\Gamma \approx 0.12$, much larger than the dispersion around mean that we find in our high redshift sample.

Figure 5 displays the relation between the rest-frame luminosity density at 2500\AA , $l_{2500\text{\AA}}$, and X-ray loudness α_{ox} . As found from earlier studies, e.g. Yuan et al. (1998b) and ?, there is a trend of AGN with higher luminosity densities at 2500\AA to be more X-ray weak then those with lower $l_{2500\text{\AA}}$. A Spearman rank order correlation test of the 15 radio-quiet AGN in our sample shows that α_{ox} and $l_{2500\text{\AA}}$ are weakly correlated with a correlation coefficient $r_s = 0.28$ and a Student's T test $T_s = 1.1$ ($P = 0.14$). The dashed lines in Figure 5 mark the mean values for the luminosity intervals of low-redshift AGN as given in Yuan et al. (1998a). Thus we see that the high-redshift quasars in our sample do not show any significant deviation from the values of low-redshift radio-quiet AGN.

In figure 6 we plot α_{ox} as a function of redshift. We do not find a correlation between the two quantities, again consistent with earlier studies (Yuan et al. 1998b; Mathur et al. 2002; ?). Recent

work by Strateva et al. (2005) has also found that the primary dependence of α_{ox} is on luminosity, rather than on redshift. The dotted line displays the mean value of $z > 2$ radio-quiet quasar sample of Yuan et al. (1998a) observed with ROSAT. The mean $\alpha_{\text{ox}} = 1.57 \pm 0.20$ of our 15 radio-quiet sources agrees with $\alpha_{\text{ox}} = 1.69 \pm 0.03$ for $z > 2$ objects in the sample of Yuan et al. (1998a). The mean and the range of α_{ox} values also are consistent with values in Strateva et al. (2005; see their figure 11, bottom).

As shown in Figure 7 radio-loud quasars are brighter by about two orders of magnitude in the 2-10 keV band than their radio-quiet cousins for a given luminosity density at 2500\AA . This result suggests that the X-ray emission of radio-loud objects is dominated by beamed emission from the jet.

5. Discussion

In this paper we present XMM detections of 16 high redshift ($z > 4$) quasar, 5 radio-loud and 11 radio-quiet. Spectral shapes were determined for 4 radio-loud and 10 radio-quiet quasars (Table 4). 5 other quasars previously detected by Chandra could not be detected by XMM. This sample is not complete; objects were chosen based on their availability in the XMM public archive. The sample of our own XMM observations was based on previous X-ray detections, though we focused on observing radio-quiet objects which are more representative ($\sim 90\%$) of the general quasar population. Nonetheless, with 14 spectroscopic observations, we are finally in a position to look for trends in the X-ray properties of high redshift quasars.

Our results presented here confirm earlier studies by e.g. Yuan et al. (1998a) and ?, that α_{ox} depends on luminosity (Figure 5) and show that there is no clear dependence of α_{ox} on redshift (Figure 6). The agreement of the mean $\alpha_{\text{ox}} = 1.57$ of our radio-quiet sources with the radio-quiet $z > 2$ sample of Yuan et al. (1998a) suggests no evolution of α_{ox} by redshift. Strateva et al. (2005) reached a similar conclusion independently. We find a mild trend of α_{ox} decreasing with α_X , but this is not a secure correlation.

High redshift radio-loud quasars are more luminous in X-rays and have flatter X-ray spectra compared to the radio-quiet quasars. This difference

in the two populations is similar to that observed in low redshift (Wilkes & Elvis 1987). Based upon studies of hardness ratios and flux estimates of a handful of sources Bechtold et al (1994) claimed that high redshift radio-loud quasars are more absorbed than their radio-quiet cousins, suggesting an intrinsic difference over and above that already present at low redshift. Elvis et al. (1994) obtained ROSAT spectra of three radio-loud and 3 radio-quiet quasars. Amongst the radio-loud objects, only one showed 3σ absorption. Statistically significant ($> 2\sigma$) intrinsic absorption is present only in 2 out of 5 radio-loud quasars in our sample. Thus, there is some evidence for the high redshift radio-loud quasars to be more absorbed than the radio-quiet quasars, even though the sample size is small; the X-ray spectra of absorbed quasars, however, appear to be dominated by the jet emission.

We find clear evidence for the 10 radio-quiet quasars with X-ray spectra in our sample to have steep spectral slopes $< \alpha_X > = 1.23 \pm 0.48$ comparable to those in NLS1 galaxies at low redshift. If we exclude SDSS J1401+0244, which may be a radio-loud quasar, the mean and standard deviation change to $< \alpha_X > = 1.33 \pm 0.38$. If we use a flatter slope for BR 0351-1034 (without intrinsic absorption), then the mean and standard deviation become $< \alpha_X > = 1.20 \pm 0.48$ for all the 10 radio-quiet sources and $< \alpha_X > = 1.30 \pm 0.44$ excluding SDSS J1401+0244. This is an exciting new result and gives credence to the hypothesis of Mathur (2000) that NLS1s are low-redshift cousins of high-redshift quasars, in that they are highly accreting and contain rapidly growing black holes. Moreover, the high Eddington luminosities independently derived for some of our targets, e.g. BRI 0103+0032, PSS J0248+1802 and BR 2237-0607, support the general result. The mean spectral slope that we find is consistent with that found by Vignali et al. (2005) and Shemmer et al. (2005) within the errors. A joint fit performed on Chandra and XMM data of eight radio-quiet $z > 4$ quasars led to an “average” $\alpha_X = 0.97^{+0.06}_{-0.04}$ by Shemmer et al. (2005). Similarly Vignali et al. performed a joint fit to 48 radio-quiet quasars and got an average $\alpha_X = 0.93^{+0.10}_{-0.09}$. We have shown above that the comparison of spectral shapes between high redshift quasars and low redshift Seyferts is not significantly affected by spec-

tral complexity of lower-luminosity Seyferts. It is very useful to make such a comparison because we have well determined Eddington luminosities only for the Seyfert population. While we are making progress in determining spectral shapes, black hole masses and Eddington luminosities in luminous quasars, these studies are still not done for well defined samples and are fraught with difficulties.

Shemmer et al. (2004) studied high redshift quasars in the redshift range $2 < z < 3.5$ and came to conclusions very similar to ours. They determined black hole masses using $H\beta$ widths for their sample objects and found them to have high Eddington luminosities, similar to NLS1s, and distinct from BLS1s. They also found that such highly accreting sources, including NLS1 have high metallicities as suggested by Mathur (2000) (see also Fields et al. 2005). Thus there appears to be mounting evidence for similarity of properties between NLS1s and high redshift quasars. Whether all luminous quasars share these properties remains to be seen.

In a recent study Piconcelli et al. (2005) performed a systematic analysis of low redshift ($z \leq 1.72$) luminous quasars from the Palomar-Green (PG) bright quasar sample. They found a mean power-law slope of $< \alpha_X > = 0.89 \pm 0.11$ for radio-quiet quasars. This slope is also statistically consistent with what we find for $z > 4$ quasars, and similar to those of NLS1s.

The above results imply that perhaps *most* luminous quasars radiate at close to Eddington luminosity, based on their X-ray spectral shape. This may not be a correct interpretation of the observations if correlation of α_X with L/L_{Edd} seen in Seyferts (e.g. Williams et al. 2004) does not extend to luminous quasars, with high mass black holes. However, there is some indication in the literature that such an interpretation may in fact be true. Corbett et al. (2003) estimated black hole masses for a large number of quasars over a range of luminosity and found that black hole mass is proportional to luminosity. This implies that the Eddington luminosity of all quasars may be similar. Given the large error in the correlation equation in Corbett et al., it is not obvious, however, what that Eddington ratio is. That they all may have high Eddington luminosity, similar to NLS1s, is only speculative at this stage (but see

Shemmer et al. 2004); we wish to draw definitive conclusions on the properties of our own sample only.

The evidence presented in this paper, and other results quoted above, support the idea that both high redshift quasars and NLS1s accrete at high Eddington rate. There is, however, one major difference in the two populations. The high redshift quasars are also very luminous objects, containing massive black holes of $\approx 10^9 M_\odot$ or so (e.g., Dietrich & Hamann 2004; Vestergaard 2004; Netzer 2003). Thus it appears that while high mass black holes accrete at high rates and grow most of their mass at high redshift, the low mass black holes, as in some NLS1s, accrete at high rate and grow most of their mass at low redshift. This scenario appears to be consistent with “anti-hierarchical” black hole growth found from the studies of X-ray background (e.g., Merloni 2004).

We would like to thank Matthias Dietrich for numerous discussions on the properties of high-redshift quasars and comments and suggestions on the manuscript. This research has made use of the NASA/IPAC Extra-galactic Database (NED) which is operated by the Jet Propulsion Laboratory, Caltech, under contract with the National Aeronautics and Space Administration.

This work was supported in part by NASA grant NAG5-9937.

REFERENCES

- Alexander, D.M., Bauer, F.E., Brandt, W.N., et al., 2003, *AJ*, 126, 539
- Avni, Y., & Tananbaum, H. 1986, *ApJ*, 305, 83
- Barger, A.J., Cowie, L.L., Brandt, W.N., Capak, P., Garmire, G.P., Hornschemeier, A.E., Steffen, A.T., & Wehner, E.H., 2002, *AJ*, 124, 1839
- Bechtold, J., Elvis, M., Fiore, F., et al., 1994, *AJ*, 108, 374
- Becker, R. H., White, R. L., & Helfand, D. J. 1995, *ApJ*, 450, 559
- Beckmann, V., Engels, D., Bade, N., & Wucknitz, O., 2003, *A&A*, 401, 927
- Boller, T., Fabian, A.C., Brandt, W.N., & Freyberg, M.J., 2000, *MNRAS*, 315, L23
- Boroson, T.A., 2002, *ApJ*, 565, 78
- Brandt, W.N., Mathur, S., & Elvis, M 1997, *MNRAS*, 285, 25
- Brandt, W.N., Guainazzi, M., Kaspi, S., Fan, X., et al., 2001a, *AJ*, 121, 591
- Brandt, W.N., Hornschemeier, A.E., Alexander, D.M., et al., 2001b, *AJ*, 122, 1
- Brandt, W.N., Schneider, D.P., Fan, X., et al., 2002a, *ApJ*, 569, L5
- Brandt, W.N., Vignali, C., Fan, X., Kaspi, S. & Schneider, D. 2002b, *MPE Report* 279, p235
- Brinkmann, W., Yuan, W., & Siebert, J., 1997, *A&A*, 319, 413
- Brocksopp, C., Puchnarewicz, E.M., Mason, K.O., Cordova, F.A.M., & Priedhorsky, W.C. 2004, *MNRAS*, 349, 687
- Bromm, V., & Larson, R.B., 2004, *ARA&A*, 42, 79
- Cappi, M., Matsuoka, M., Comastri, A., Brinkmann, W., Elvis, M., Palumbo, G.G.C., & Vignali, C., 1997, *ApJ*, 478, 492
- Cheung, C.C., 2004, *ApJ*, 600, L23
- Castander, F.J., Treister, E., Maccarone, T.J., Coppi, P.S., Maza, J., Zepf, S., & Guzman, R., 2003, *AJ*, 125, 1689
- Corbett, E.A., et al., 2003, *MNRAS*, 343, 705
- Condon, J. J., Cotton, W. D., Greisen, E. W., Yin, Q. F., Perley, R. A., Taylor, G. B., & Broderick, J. J., 1998, *AJ*, 115, 1693.
- Dickey, J.M., Lockman, F.J., 1990, *ARA&A*, 28, 215
- Dietrich, M., Appenzeller, I., Vestergaard, M., & Wagner, S.J., 2002a, *ApJ*, 564, 2002
- Dietrich, M., Hamann, F., Shields, J.C., Constantin, A., Vestergaard, M., Chaffee, F., Foltz, C.B., & Junkkarinen, V.T., 2002b, *ApJ*, 581, 912
- Dietrich, M., Hamann, F., Appenzeller, I., & Vestergaard, M., 2003, *ApJ*, 596, 817

- Dietrich, M., & Hamann, F., 2004, *ApJ*, 611, 761
- Di Matteo, T., Croft, R.A.C., Springel, V., & Hernquist, L., 2004, *ApJ*, 610, 80
- Durret, F., Lima Neto, G.B., & Forman, W., 2005, *A&A*, in press, astro-ph/0411527
- Elvis, M., Fiore, F., Wilkes, B.J., & McDowell, J., 1994, *ApJ*, 422, 60
- Fabian, A.C., Brandt, W.N., McMahon, R.G., & Hook, I.M., 1997, *MNRAS*, 291, L5
- Fabian, A.C., Iwasawa, K., Celotti, A., Brandt, W.N., McMahon, R.G., & Hook, I.M., 1998, *MNRAS*, 295, L25
- Fabian, A.C., Celotti, A., Iwasawa, K., et al., 2001, *MNRAS*, 323, 373
- Fan, X., et al., *AJ*, 120, 1167
- Farrah, D., Priddey, R., Wilman, R., Haehnelt, M., & McMahon, R., 2004, *ApJ*, 611, L13
- Ferrarese, L., & Merritt, D., 2000, *ApJ*, 539, L9
- Ferrero, E., & Brinkmann, W., 2003, *A&A* 402, 465
- Fields, D.L., Mathur, S., Pogge, R.W., Nicastro, F., Komossa, S., & Krongold, Y., 2005, *ApJ* submitted, astro-ph/0504159
- Gebhardt, K., Kormendy, J., Ho, L.C., et al., 2000, *ApJ*, 543, L5
- Giacconi, R., Zirm, A., Wang, J., et al., 2002, *ApJS*, 139, 369
- Granato, G.L., De Zotti, G., Silva, L., Bressan, A., & Danese, L., 2004, *ApJ*, 600, 580
- Grupe, D., 1996, PhD Thesis, Universität Göttingen
- Grupe, D., 2004, *AJ*, 127, 1799
- Grupe, D., Mathur, S., & Elvis, M., 2003, *AJ*, 126, 1159
- Grupe, D., Mathur, S., Wilkes, B.J., & Elvis, M., 2004, *AJ*, 127, 1
- Grupe, D., & Mathur, S., 2004, *ApJ*, 606, L41
- Hasinger, G., Burg, R., Giacconi, R., Schmidt, M., Trümper, J., & Zamorani, G., 1998, *A&A*, 329, 482
- Henry, J.P., Giola, I.M., Böringer, H., et al., 1994, *AJ*, 107, 1270
- Hogg, D., 1999, astro-ph/9905116
- Hook, I.M., & McMahon, R.G., 1998, *MNRAS*, 294, L7
- Irwin, M., McMahon, R.G., & Hazard, C., 1991, in Crampton, D., *ASP Conference Series*, Vol 21, 'The Space Distribution of Quasars', p117
- Isaak, K.G., McMahon, R.G., Hills, R.E., & Withington, S., 1994, *MNRAS*, 269, L28
- Jansen, F., Lumb, D., Altieri, B., et al., 2001, *A&A*, 365, L1
- Kaspi, S., Brandt, W.N., & Schneider, D.P., 2000a, *AJ*, 119, 2031
- Kaspi, S., Smith, P.S., Netzer, H., Moaz, D., Januzzi, B.T., & Givon, U., 2000b, *ApJ*, 533, 631
- Kellermann, K.I., Sramek, R., Schmidt, M., Shaffer, D.B., & Green, R., 1989, *AJ*, 98, 1195
- Kennefick, J.D., De Carvalho, R.R., Djorgovski, S.G., Wilber, M.M., Dickson, E.S., Weir, N., Fayyad, U., & Roden, J., 1995, *AJ*, 110, 78
- Leighly, K.M., 1999, *ApJS*, 125, 297
- Mathur, S., 2000, *MNRAS*, 314, L17
- Mathur, S., & Elvis, M., 1995, *AJ*, 110, 1551
- Mathur, S., Wilkes, B.J., & Ghosh, H., 2002, *ApJ*, 570, L5
- Mathur, S., & Grupe, D., 2005, *A&A*, 432, 463
- Mathur, S., & Grupe, D., 2005, *ApJ*, in press.
- Merloni, A., 2004, *MNRAS*, 353, 1035
- Netzer, H., 2003, *ApJ*, 583, L5
- Merritt, D., & Ferrarese, L., 2001, *ApJ*, 547, 140
- Osterbrock, D.E., & Pogge, R.W., 1985, *ApJ*, 297, 166

- Péroux, C., Storrie-Lombardi, McMahon, R.G., Irwin, M., & Hook, I.M., 2001, *AJ*, 121, 1799
- Petric, A.O., Carilli, C.L., Bertoldi, F., Fan, X., Cox, P., Strauss, M.A., & Schneider, D.P., 2003, *AJ*, 126, 15
- Pfeffermann, E., Briel, U.G., Hippmann, H., et al., 1987, *SPIE*, 733, 519
- Piconcelli, E., Jimenez-Bailón, E., Guainazzi, M., Schartel, N., Rodríguez-Pascual, P. M., & Santos-Lleó, M., 2005, *A&A*, 432, 15
- Schneider, D.P., Schmidt, M., Hasinger, G., Lehmann, I., Gunn, J.E., Giacconi, R., Trümper, J., & Zamorani, G., 1998, *AJ*, 115, 1230
- Schneider, D.P., Fan, X., Hall, P.B., et al., 2003, *AJ*, 126, 2579
- Siemiginowska, A., Smith, R.K., Aldcroft, T.L., Schwartz, D.A., Paerels, F., Petric, A.O., 2003, *ApJ*, 598, L15
- Shemmer, O., Netzer, H., Maiolino, R., Oliva, E., Croom, S., Corbett, E., & di Fabrizio, L., 2004, *ApJ*, 614, 547
- Shemmer, O., Brandt, W.N., Vignali, C., Schneider, D.P., Fan, X., Richanrds, G.T., & Strauss, M.A., 2005, *ApJ*, accepted, astrp-ph/0505482
- Silverman, J.D., Green, P.J., Kim, D.-W., et al., 2002, *ApJ*, 569, L1
- Smith, J.D. et al. 1994 *AJ*, 108, 1147
- Stern, D., Djorgovski, S.G., Perley, R.A., DeCavalho, R.R., & Wall, J.V., 2000, *AJ*, 119, 1526
- Storrie-Lombardi, L.J., McMahon, R.G., Irwin, M.J., & Hazard, C., 1996b, *ApJ*, 468, 121
- Strateva, I.V., Brandt, W.N., Schneider, D.P., Vanden Berk, D.G., & Vignali, C., 2005, *AJ*, 130, 387
- Strüder, L., Briel, U., Dennerl, K., et al., 2001, *A&A*, 365, L18
- Sulentic, J.W., Stripe, G.M., Marziani, P., Zamanov, R., Calvani, M., & Braitto, V., 2004, *A&A*, 423, 121
- Tananbaum, Avni, Y., Branduardi, G., et al., 1979, *ApJ*, 234, L9
- Trümper, J., 1982, *Adv. Space Res.*, 4, 241
- Turner, M.J.L., Abbey, A., Arnaud, M., et al., 2001, *A&A*, 365, L27
- Vanden Berk, D.E., et al., 2001, *AJ*, 122, 549
- Vestergaard, M., 2002, *ApJ*, 571, 733
- Vestergaard, M., 2004, *ApJ*, 601, 676
- Vignali, C., Brandt, W.N., Fan, X., Gunn, J.E., Kaspi, S., Schneider, D.P., & Strauss, M.A., 2001, *AJ*, 122, 2155
- Vignali, C., Bauer, F.E., Alexander, D.M., Brandt, W.N., Hornschemeier, A.E., Schneider, D.P., & Garmire, G.P., 2002, *ApJ*, 580, L105
- Vignali, C., Brandt, W.N., Schneider, D.P., Garmire, G.P., & Kaspi, S., 2003, *AJ*, 125, 418
- Vignali, C., Brandt, W.N., Schneider, D.P., & Kaspi, S., 2005, *AJ*, 129, 2519
- Voges, W., Aschenbach, B., Boller, T., et al., 1999, *A&A*, 349, 389
- Wilkes, B.J., & Elvis, M., 1987, *ApJ*, 323, 243
- Wilkes, B.J., Tananbaum, H., Worrall, D.M., Avni, Y., Oey, M.S., & Flanagan, J., 1994, *ApJS*, 92, 53
- Wilkes, B.J., et al., 2001, *ASP Conf. Ser.* 232, *The New Era of Wide Field Astronomy*, eds. R.G. Clowes, A.J., Adamson, & G.E. Bromage (San Francisco, ASP), 47
- Williams, R.J., Mathur, S., & Pogge, R.W., 2004, *ApJ*, 610, 737
- Worsley, M.A., Fabian, A.C., Turner, A.K., Celotti, A., & Iwasawa, K., 2004a, *MNRAS*, 350, 207
- Worsley, M.A., Fabian, A.C., Celotti, A., & Iwasawa, K., 2004b, *MNRAS*, 350, 67
- Worsley, M.A., Fabian, A.C., Barcons, X., Mateos, S., Hasinger, G., & Brunner, H., 2004c, *MNRAS*, 352, L28
- York, D.G., et al., 2000, *AJ*, 120, 1579

- Yuan, W., Brinkmann, W., Siebert, J., & Wang, W., 1998a, A&A, 330, 108
- Yuan, W., Siebert, J., & Brinkmann, W., 1998b, A&A, 334, 498
- Yuan, W., Fabian, A.C., Celotti, A., Jonker, P.G., 2003, MNRAS, 346, L7
- Yuan, W., Matsuoka, M., Wang, T., Ueno, S., Kubo, H., & Mihara, T., 2000, ApJ, 545, 625
- Yuan, W., Fabian, A.C., Celotti, A., McMahon, R.G., Matsuoka, M., 2005, MNRAS, 358, 432
- Zickgraf, F.-J., Voges, W., Krauter, J., Thiering, I., Appenzeller, I., Mujica, R., & Serrano, A., 1997, A&A, 323, L21
- Zimmermann, U., Boese, G., Becker, W., et al., 1998, 'EXSAS User's Guide', MPE report (<http://wave.xray.mpe.mpg.de/exsas/users-guide>)

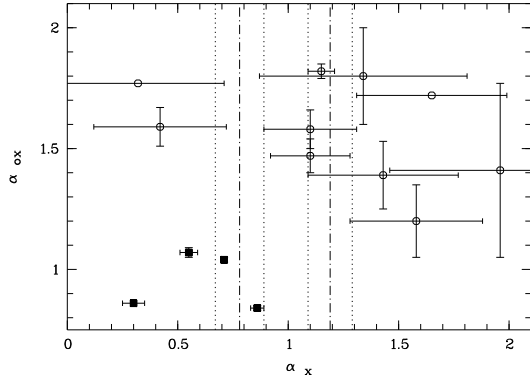


Fig. 4.— X-ray spectral slope α_X vs. α_{ox} . Symbols are as defined in Figure 5. The dashed-dotted lines shows the mean values of 2-10 keV α_X of low-redshift BLS1s and NLS1s ($\alpha_X=0.78$ and 1.19 respectively) as given in Leighly (1999). The dotted lines mark the standard deviations around the mean.

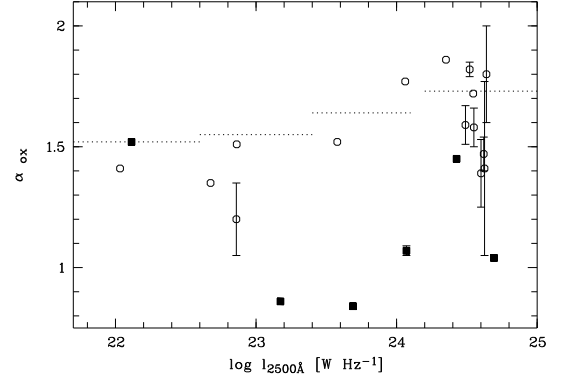


Fig. 5.— Luminosity density at 2500Å vs. α_{ox} . Radio-loud quasars are displayed as filled squares and radio-quiet quasars as open circles. For objects without error bars, α_{ox} was taken from the literature as given in Table 4. The dashed lines display the α_{ox} of low-redshift AGN as given in Yuan et al. (1998a).

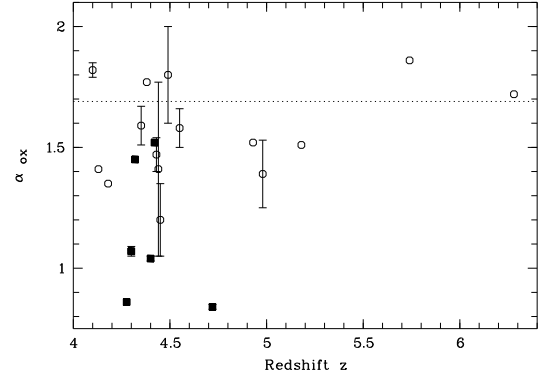


Fig. 6.— Redshift z vs. α_{ox} . Symbols are as defined in Figure 5. The dotted line displays the mean value of $Z>2$ quasars in the sample of Yuan et al. (1998a).

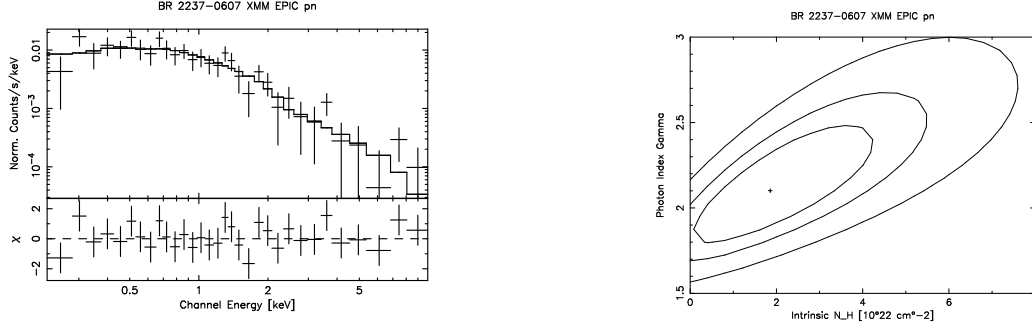


Fig. 1.— Power-law fit with neutral galactic absorption (fixed to galactic value) and intrinsic absorption with metal abundance = solar to the EPIC pn of BR 2237–0607. The left panel shows the fit to the pn data and the right one the contour plot between the Photon spectral index Γ and the intrinsic column density N_{H} .

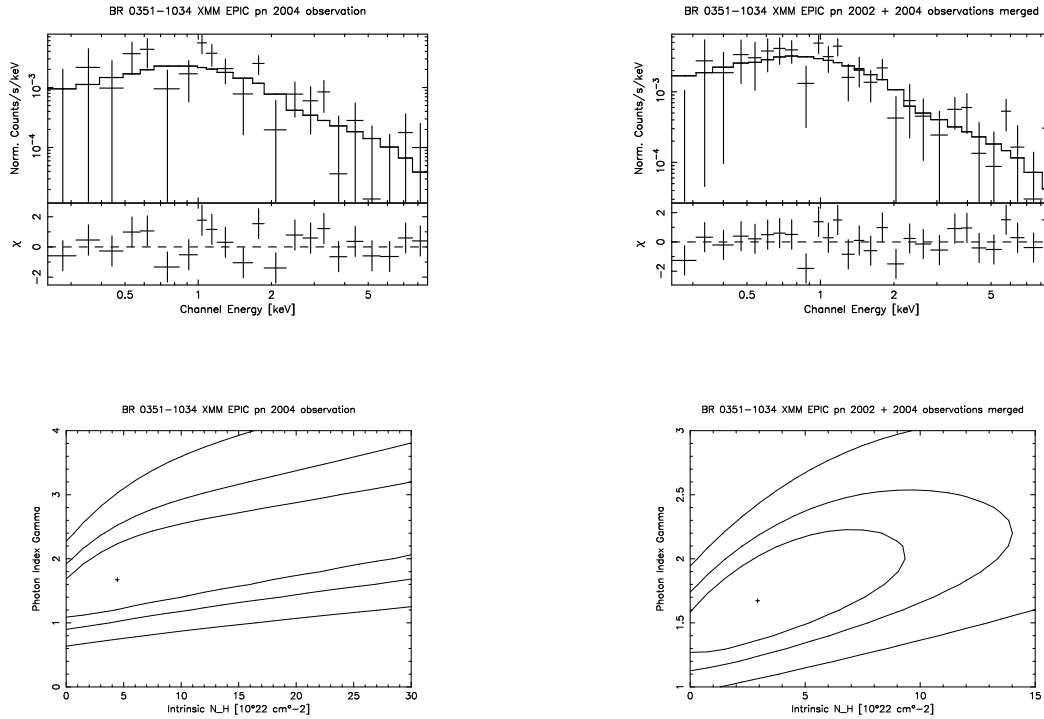


Fig. 2.— Power-law fit with neutral galactic absorption (fixed to galactic value) and intrinsic absorption with metal abundance = solar to the EPIC pn of BR 0351–1034. The left panels shows the fit to the 2004 January pn data and the right ones the fit to the merged data of the 2002 and 2004 observations. The upper panels show the spectral fits to the data and the lower panels the contours with the Photon spectral index Γ and the intrinsic absorption parameter N_{H} .

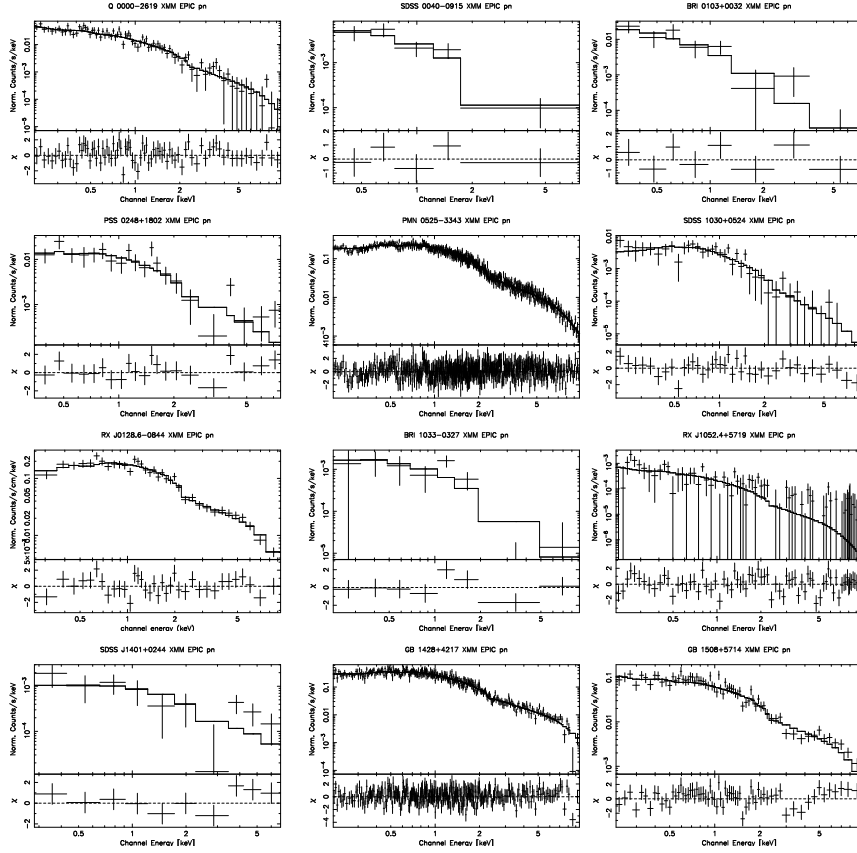


Fig. 3.— Best fits to the XMM EPIC pn spectra of the high redshift quasars with XMM observations as listed in Table 4.

TABLE 1
z>4.0 QSOs WITH XMM OBSERVATIONS

No.	Object	α_{J2000}	δ_{J2000}	z	XMM Obs-ID	UT date	T_{acc}^1	Counts	XMM-Newton reference
1	Q 0000-2619	00 03 22.92	-26 03 18.7	4.100	0103060301	2002 Jun 25	37.8	1366±46	Ferrero & Brinkmann (2003)
2	SDSS 0040-0915	00 40 54.65	-09 15 26.8	4.980	0065140101	2002 Jan 07	3.4	49±8	Schneider et al. (2003)
3	BRI 0103+0032	01 06 19.20	+00 48 23.3	4.440	0150870201	2003 Jul 15	3.7	53±11	—
4	PSS J0248+1802	02 48 54.30	+18 02 49.2	4.422	0150870301	2003 Feb 14	7.4	161±16	—
5	BR 0351-1034	03 53 46.91	-10 25 19.0	4.351	²	²	39.1	254±30	Grupe et al. (2004)
6	PMN J0525-3343	05 25 06.17	-33 43 05.3	4.400	³	³	72.9	28809±177	Worsley et al. (2004a)
7	RX J1028.6-0844	10 28 37.70	-08 44 23.6	4.276	0093160701	2002 May 15	4.4	1809±44	Grupe et al. (2004)
8	SDSS 1030+0524	10 30 27.10	+05 24 55.00	6.28	0148560501	2003 May 22	67.5	342±33	Farrah et al. (2004)
9	BRI 1033-0327	10 36 23.80	-03 43 19.3	4.49	0150870401	2002 Dec 20	26.5	56±14	—
10	SDSS 1044-0125	10 44 33.04	-01 25 02.2	5.740	0125300101	2000 May 28	34.1	32±9	Brandt et al. (2001a)
11	RX J1052.4+5719	10 52 25.90	+57 19 07.0	4.450	⁴	⁴	535.7 ⁴	368±52	Worsley et al. (2004c)
12	VLA J1236+6213	12 36 42.00	+62 13 31.0	4.420	⁵	⁵	205 ⁵	—	—
13	CXOHDFN J123647+620941	12 36 47.90	+62 09 41.0	5.180	⁵	⁵	205 ⁵	—	—
14	CXOHDFN J123719+621025	12 37 19.00	+62 10 25.0	4.130	⁵	⁵	205 ⁵	—	—
15	CXOCY J125304-090737	12 53 04.00	-09 07 37.0	4.180	0112270701	2003 Jan 15	8.1	—	—
16	SDSS J1401+0244	14 01 46.53	+02 44 34.7	4.380	0098010101	2000 Jun 28	32.7	115±20	Schneider et al. (2003)
17	GB 1428+4217	14 30 23.78	+42 04 26.3	4.720	⁶	⁶	14.2	8476±92	Worsley et al. (2004b)
18	GB 1508+5714	15 10 02.23	+57 03 04.9	4.300	0111260201	2002 May 11	9.4	1437±39	—
19	RX J1759.4+6638	17 59 27.76	+66 38 53.6	4.320	⁷	⁷	6.9	12±7	—
20	CXOMP J213945-234655	21 39 45.00	-23 46 55.0	4.930	0008830101	2001 Apr 29	11.5 ⁸	—	—
21	BR 2237-0607	22 39 53.57	-05 52 20.0	4.558	0149410401	2003 May 17	23.1	381±29	This paper

¹Accepted GTI screened exposure times given in ks.

²Merged event file from observation IDs 0093160201 & 0203460201 (orbits 495 & 759; 2002-08-23 & 2004-01-31)

³Merged event file from the observations as listed in Table 5

⁴Merged event file from the observations as listed in Table 6; Note: the exposure time is not derived from the exposure map

⁵Merged event file from the observations as listed in Table 7; Note: the exposure time is not derived from the exposure map

⁶Merged event file from observation IDs 0111260101 & 0111260701 (orbits 549 & 569; 2002-12-09 & 2003-01-17)

⁷Merged event file from observation IDs 0112310401 & 0112310801 (orbits 457 & 523; 2002-06-08 & 2002-10-18)

⁸Note: the exposure time is not derived from the exposure map

TABLE 2
SPECTRAL FIT PARAMETERS TO THE EPIC PN DATA OF BR 2237–0607

XSPEC Model	$N_{\text{H,gal}}$ 10^{20}cm^{-2}	$N_{\text{H,intr}}$ 10^{22}cm^{-2}	α_{X}	χ^2 (DOF)
1	8.89 ± 4.32	—	1.17 ± 0.29	21.1 (29)
1	3.84 (fix)	—	0.84 ± 0.14	26.1 (30)
2	3.84 (fix)	1.84 ± 1.50	1.10 ± 0.23	23.1 (29)

(1) Power-law with Galactic absorption; (2) Power-law with Galactic absorption, and redshifted neutral absorption at $z=4.558$;

TABLE 3
SPECTRAL FIT PARAMETERS TO THE EPIC PN DATA OF BR 0351–1034

Obs. Date	XSPEC Model	$N_{\text{H,gal}}$ 10^{20}cm^{-2}	$N_{\text{H,intr}}$ 10^{22}cm^{-2}	$\alpha_{\text{X,soft}}$	$\alpha_{\text{X,hard}}$	χ^2 (DOF)
2004 Jan	1	15.3 ± 14.5	—	—	0.81 ± 0.61	6.8 (14)
	2	4.08 (fix)	—	—	0.37 ± 0.26	7.9 (15)
	3	4.08 (fix)	5.34 ± 4.30	—	0.75 (fix)	6.5 (15)
Merged 2002+2004	1	10.26 ± 8.51	—	—	0.69 ± 0.37	22.5 (25)
	2	4.08 (fix)	—	—	0.42 ± 0.17	23.5 (26)
	3	4.08 (fix)	<6.3	—	0.67 ± 0.30	22.0 (25)
	4	4.08 (fix)	—	3.50 (fix) ¹	0.42 ± 0.18	22.3 (26)
Simultaneous fit ²	1	9.65 ± 8.09	—	—	0.82 ± 0.39	29.8/33
	2	4.08 (fix)	—	—	0.55 ± 0.13	30.8/34
	3	4.08 (fix)	<2.15	—	0.76 ± 0.31	29.8/33

(1) Power-law with absorption parameter free (2) Power-law with Galactic absorption $4.08 \times 10^{20} \text{ cm}^{-2}$; (3) Power-law with Galactic absorption, and redshifted neutral absorption at $z=4.351$; (4) Broken power-law with Galactic absorption

¹ $\alpha_{\text{X,soft}}$ refers to the soft X-ray spectral slope that is suggested by fits to the ROSAT data, that suggest a break at 0.45 keV (Grupe et al. 2004)

²Simultaneous fit to the 2002 August and 2004 January data in XSPEC

TABLE 4

RESULTS OF POWER LAW FITS WITH GALACTIC (AND INTRINSIC) ABSORPTION TO THE XMM PN DATA OF $z > 4.0$ QSOs AS LISTED IN TABLE 1. FLUXES AND LUMINOSITIES ARE GIVEN IN THE REST-FRAME.

No.	Object	RL/RQ ¹	$N_{\text{H,gal}}^2$	$N_{\text{H,intr}}^2$	α_{X}	χ^2/ν	$\log F_{2-10}^3$	$\log L_{2-10}^3$	$\log l_{2500\text{\AA}}^3$	α_{ox}	Comments
1.	Q 0000-2619	RQ	1.67	—	1.15 ± 0.06	75/80	-16.33	38.83	24.52	1.82 ± 0.03	Gal * Powl
2	SDSS 0040-0915	RQ	3.37	—	1.43 ± 0.34	2/3	-16.59	38.76	24.60	1.39 ± 0.14	Gal * Powl
3	BRI 0103+0032	RQ	3.19	—	1.96 ± 0.50	5/6	-16.70	38.54	24.63	1.41 ± 0.36	Gal * Powl
4	PSS J0248+1802	RQ	9.18	—	1.10 ± 0.18	16/13	-16.36	38.88	24.62	1.47 ± 0.07	Gal * Powl
5	BR 0351-1034	RQ	4.08	—	0.42 ± 0.17^4	23/15	-17.10 ⁴	38.13 ⁴	24.49	1.59 ± 0.08^4	(Gal + Intr) * Powl
6	PMN J0525-3343	RL	2.21	1.56 ± 0.10	0.71 ± 0.01	601/600	-15.24	39.98	24.68	1.04 ± 0.01	(Gal + Intr) * Powl
7	RX J1028.6-0844	RL	4.59	0.07 ± 0.01	0.30 ± 0.05	92/84	-15.32	39.88	23.17	0.86^4	(Gal + Intr) * Powl
8	SDSS 1030+0524	RQ	3.20	6.51 ± 3.74	1.65 ± 0.34	32/39	-16.83	38.76	24.55	1.72^5	(Gal + Intr) * Powl
9	BRI 1033-0327	RQ	4.79	—	1.34 ± 0.47	8/6	-17.50	37.75	24.68	1.80 ± 0.20	Gal * Powl
10	SDSS 1044-0125	RQ	4.19	—	—	—	-17.54 ⁶	37.96 ⁶	24.35	1.86^6	XMM detection
11	RX J1052.4+5719	RQ	0.56	—	1.58 ± 0.30	73/73	-17.96	37.28	22.86	1.20 ± 0.15	Gal * Powl
12	VLA J1236+6213	RL	1.49	—	—	—	-18.92 ⁷	36.74 ⁷	22.11	1.52^7	No XMM detection
13	CXOHDFN J123647+620941	RQ	1.48	—	—	—	-18.38 ⁷	37.02 ⁷	22.86	1.51^7	No XMM detection
14	CXOHDFN J123719+621025	RQ	1.29	—	—	—	-18.54 ⁷	36.63 ⁷	22.03	1.41^7	No XMM detection
15	CXOCY J125304-090737	RQ	2.96	—	—	—	-17.65 ⁸	37.53 ⁸	22.68	1.35^8	No XMM detection
16	SDSS J1401+0244	RQ	2.36	—	0.32 ± 0.39	9/8	-17.09	38.13	24.06	1.77^9	Gal * Powl
17	GB 1428+4217	RL	1.40	2.13 ± 0.23	0.86 ± 0.03	299/310	-15.09	40.21	23.69	0.84 ± 0.01	(Gal + Intr) * Powl
18	GB 1508+5714	RL	1.47	—	0.55 ± 0.04	75/66	-15.77	39.43	24.07	1.07 ± 0.02	Gal * Powl
19	RX J1759.4+6638	RL	4.23	—	—	—	-16.29 ¹⁰	38.92 ¹⁰	24.43	1.45^{10}	XMM detection
20	CXOMP J213945-234655	RQ	3.55	—	—	—	-17.59 ¹¹	37.76 ¹¹	23.58	1.52^{11}	No XMM detection
21	BR 2237-0607	RQ	3.84	1.84 ± 1.50	1.10 ± 0.23	23/29	-16.58	38.68	24.55	1.58 ± 0.08	(Gal + Intr) * Powl

¹Radio-loud (RL) and Radio-quiet (RQ) using the definition of Kellermann et al. (1989). References on the radio-loudness are given in Section 3.3.

²Galactic column density $N_{\text{H,gal}}$ in units of 10^{20} cm^{-2} , and intrinsic column density $N_{\text{H,intr}}$ in units of 10^{22} cm^{-2}

³Rest-frame unabsorbed flux $F_{2-10 \text{ keV}}$ in units of W m^{-2} , luminosity $L_{2-10 \text{ keV}}$ in units of W, and luminosity density at 2500Å given in units of W Hz^{-1} . References for the luminosity density at 2500Å are given for each individual object in Section 3.3.

⁴Estimated from the merged 2002 and 2004 spectra

⁵ α_{ox} from Mathur et al. (2002)

⁶Based on the data given in Brandt et al. (2001a) converted into flux using PIMMS and α_{ox} taken from Brandt et al. (2001a).

⁷Flux and luminosities values from the Chandra ACIS-S count rates and X-ray slopes given in Vignali et al. (2002) and α_{ox} taken from Vignali et al. (2002).

⁸Estimated from the Chandra ACIS-S flux and X-ray slope given in Castander et al. (2003) and α_{ox} taken from Castander et al. (2003).

⁹ α_{ox} taken from Schneider et al. (2003).

¹⁰Estimated from the ROSAT PSPC flux and X-ray slope given in Kaspi et al. (2000a) and α_{ox} taken from Kaspi et al. (2000a).

¹¹Estimated from the Chandra flux given in Silverman et al. (2002) and α_{ox} from Silverman et al. (2002)

TABLE 5
XMM EPIC PN OBSERVATIONS OF PMN J0525–3343 (WORSLEY ET AL. 2004A)

Orbit	Obs ID	UT Obs. Date	T_{obs} [ks] ¹
216	0050150101	2001 Feb 11	9.8
324	0050150301	2001 Sep 15	20.2
583	0149500601	2003 Feb 02	9.2
588	0149500701	2003 Feb 24	9.3
593	0149500801	2003 Mar 06	9.0
598	0149500901	2003 Mar 16	7.6
671	0149501201	2003 Aug 08	7.6

¹screened Good Time Intervals

TABLE 6
XMM OBSERVATIONS OF RX J1052.4+5719 WITH THE PN AND MEDIUM FILTER

Orbit	Obs ID	UT Obs. Date	T_{obs} [ks] ¹
344	0022740101	2001 Oct 25	14.6
345	0022740201	2001 Oct 27	38.6
349	0022740301	2001 Nov 04	31.9
524	0147510901	2002 Oct 19	57.9
525	0147511001	2002 Oct 21	73.8
526	0147511101	2002 Oct 23	53.0
544	0147511601	2002 Nov 27	97.9
547	0147511701	2002 Dec 04	88.5
548	0147511801	2002 Dec 06	79.5

¹screened Good Time Intervals

TABLE 7
XMM OBSERVATIONS OF VLA J1236+6213, CXOHDFN J123647+6209, AND CXOHDFN J123719+6210 WITH THE PN AND THIN FILTER

Orbit	Obs ID	UT Obs. Date	T_{obs} [ks] ¹
264	0111550101	2001-05-18	37.5
264	0111550201	2001-05-19	35.1
268	0111550301	2001-05-27	23.8
271	0111550401	2001-06-01	81.0
725	0162160201	2003-11-24	10.5
731	0162160401	2003-12-06	8.1
735	0162160601	2003-12-14	9.2

¹screened Good Time Intervals

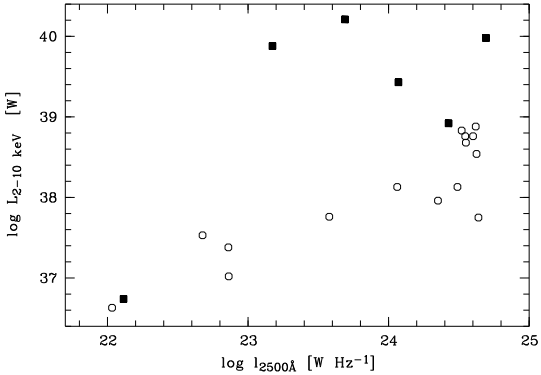


Fig. 7.— Rest-frame luminosity density at 2500\AA $\log l_{2500\text{\AA}}$ vs. rest-frame 2-10 keV X-ray luminosity $\log L_{2-10\text{ keV}}$. Symbols are as defined in Figure 5.